Acta Crystallographica Section B
Structural Science
ISSN 0108-7681

Polymorphs of *p*-nitrophenol as studied by variable-temperature X-ray diffraction and calorimetry: comparison with *m*-nitrophenol

Grażyna Wójcik* and Izabela Mossakowska

Institute of Physical and Theoretical Chemistry, Wrocław University of Technology, Wyb. Wyspiańskiego 27, 50-370 Wrocław, Poland

Correspondence e-mail: grazyna.m.wojcik@pwr.wroc.pl

Received 22 July 2005
Accepted 21 October 2005

Crystal structures of two polymorphic forms of *p*-nitrophenol have been determined at several temperatures between 120 and 375 K. The thermal expansion tensor has been determined for both polymorphs. The rigid-body mean-square amplitudes of molecular translations and librations and the amplitudes of the internal torsions of the nitro group have been calculated at different temperatures. Differential scanning calorimetry was used to find the temperature and enthalpy of the polymorphic transformation. The results were compared with those recently obtained for *m*-nitrophenol polymorphs. Some conclusions concerning the polymorphism of *p*- and *m*-nitrophenols are presented.

1. Introduction

Polymorphism is defined as the occurrence of two or more different crystal structures for the same compound. The investigation of polymorphic structures enables the crystal structure *versus* property relationship to be studied. On the other hand, the analysis of the crystal structures of isomers may give insight into the mutual dependence between molecular and crystal structures. A comparison of the polymorphic structures of *para*- and *meta*-nitrophenol provides an opportunity to explore and to advance our understanding of both problems. Polymorphic structures may be less or more similar depending on the compound. Isostructurality refers to the similarity of molecular arrangements in the crystals of different compounds. Isostructurality does not depend on unit-cell parameters or space group, thus it ought not be mistaken for isomorphism. The similarity of polymorphic structures has recently been depicted through one-, two- or three-dimensional isostructurality (Fábián & Kalman, 2004).

The objective of this work has been to study the polymorphic crystal structures of *p*-nitrophenol over a wide temperature range. Thermal expansion and atomic displacement parameters analysed within the TLS formalism (Cruickshank, 1956; Schomaker & Trueblood, 1968; Dunitz & White, 1973; Dunitz *et al.*, 1988; Schomaker & Trueblood, 1998) have been explored to gain insight into the molecular interactions and motions, including their thermal evolution. The differential scanning calorimetry (DSC) measurements have been undertaken to determine the temperature and enthalpy of the β to α phase transition. The problem of persistent metastability of the α crystal will be discussed in terms of the intermolecular interactions in the crystal.

The other objective of the work has been the comparison of crystal structures, molecular dynamics from rigid-body analysis and the thermodynamic stability of two *p*-nitrophenol polymorphs with those corresponding to the polymorphs of the *meta* isomer, *i.e.* *m*-nitrophenol, studied recently by us

Table 1
Experimental details for the α and β polymorphs of *p*-nitrophenol at three chosen temperatures.

	α at 120 K	α at room temperature	α at 333 K
Crystal data			
Chemical formula	$C_6H_5NO_3$	$C_6H_5NO_3$	$C_6H_5NO_3$
M_r	139.11	139.11	139.11
Cell setting, space group	Monoclinic, $P2_1/c$	Monoclinic, $P2_1/c$	Monoclinic, $P2_1/c$
a, b, c (Å)	6.136 (1), 8.800 (1), 11.481 (3)	6.138 (2), 8.874 (3), 11.702 (3)	6.146 (1), 8.903 (2), 11.763 (5)
β (°)	103.40 (2)	103.05 (2)	103.09 (3)
V (Å^3)	603.1 (2)	620.9 (3)	626.9 (3)
Z	4	4	4
D_x (Mg m^{-3})	1.532	1.488	1.474
Radiation type	Mo $K\alpha$	Mo $K\alpha$	Mo $K\alpha$
No of reflections for cell parameters	1206	532	665
θ range (°)	4.05–27.1	4.12–20.42	3.97–21.73
μ (mm^{-1})	0.13	0.12	0.12
Temperature (K)	120 (2)	298 (2)	333 (2)
Crystal form, colour	Thin plate, pale yellow	Thin plate, pale yellow	Thin plate, pale yellow
Crystal size (mm)	0.79 × 0.55 × 0.50	0.77 × 0.38 × 0.38	0.79 × 0.50 × 0.55
Data collection			
Diffractometer	KUMA Diffraction KM4CCD	KUMA Diffraction KM4CCD	KUMA Diffraction KM4CCD
Data collection method	ω scans	ω scans	ω scans
Absorption correction	None	None	None
No of measured, independent and observed reflections	1872, 1019, 906	2165, 1197, 897	2046, 1067, 725
Criterion for observed reflections	$I > 2\sigma(I)$	$I > 2\sigma(I)$	$I > 2\sigma(I)$
R_{int}	0.046	0.039	0.029
θ_{max} (°)	27.04	27.36	27.42
Range of h, k, l	$-3 \Rightarrow h \Rightarrow 7$ $-11 \Rightarrow k \Rightarrow 11$ $-14 \Rightarrow l \Rightarrow 6$	$-7 \Rightarrow h \Rightarrow 7$ $-11 \Rightarrow k \Rightarrow 4$ $-13 \Rightarrow l \Rightarrow 15$	$-4 \Rightarrow h \Rightarrow 7$ $-11 \Rightarrow k \Rightarrow 11$ $-14 \Rightarrow l \Rightarrow 7$
Refinement			
Refinement on	F^2	F^2	F^2
$R\,[F^2 > 2\sigma(F^2)]$, $wR\,(F^2)$, S	0.033, 0.095, 1.08	0.047, 0.138, 1.08	0.048, 0.167, 1.09
No of reflections	1019	1197	1067
No. of parameters	112	96	112
H-atom treatment	Mixture of independent and constrained refinement	Mixture of independent and constrained refinement	Mixture of independent and constrained refinement
Weighting scheme	$w = 1/[\sigma^2(F_o^2) + (0.0474P)^2 + 0.2271P]$, where $P = (F_o^2 + 2F_c^2)/3$	$w = 1/[\sigma^2(F_o^2) + (0.0728P)^2 + 0.05P]$, where $P = (F_o^2 + 2F_c^2)/3$	$w = 1/[\sigma^2(F_o^2) + (0.0900P)^2 + 0.0545P]$, where $P = (F_o^2 + 2F_c^2)/3$
$(\Delta/\sigma)_{max}$	0.001	< 0.000	0.016
$\Delta\rho_{max}$, $\Delta\rho_{min}$ (e Å^{-3})	0.21, −0.21	0.16, −0.13	0.16, −0.12
Extinction method	*SHELXL*97	*SHELXL*97	*SHELXL*97
Extinction coefficient	0.063 (8)	0.069 (1)	0.095 (19)

	β at 120 K	β at room temperature	β at 375 K
Crystal data			
Chemical formula	$C_6H_5NO_3$	$C_6H_5NO_3$	$C_6H_5NO_3$
M_r	139.11	139.11	139.11
Cell setting, space group	Monoclinic, $P2_1/n$	Monoclinic, $P2_1/n$	Monoclinic, $P2_1/n$
a, b, c (Å)	3.6780 (10), 11.091 (2), 14.627 (3)	3.7740 (10), 11.147 (4), 14.695 (3)	3.8310 (10), 11.093 (2), 14.835 (3)
β (°)	92.75 (2)	92.60 (2)	93.45 (3)
V (Å^3)	596.0 (2)	617.6 (3)	629.3 (2)
Z	4	4	4
D_x (Mg m^{-3})	1.550	1.496	1.468
Radiation type	Mo $K\alpha$	Mo $K\alpha$	Mo $K\alpha$
No of reflections for cell parameters	796	805	1153
θ range (°)	3.9–25.3	4.0–22.5	3.6–22.9
μ (mm^{-1})	0.13	0.12	0.12
Temperature (K)	120 (2)	293 (2)	375 (2)
Crystal form, colour	Needle, pale yellow	Needle, pale yellow	Needle, pale yellow
Crystal size (mm)	0.57 × 0.55 × 0.53	0.82 × 0.36 × 0.25	0.98 × 0.53 × 0.45
Data collection			
Diffractometer	KUMA Diffraction KM4CCD	KUMA Diffraction KM4CCD	KUMA Diffraction KM4CCD
Data collection method	ω scans	ω scans	ω scans
Absorption correction	None	None	None
No of measured, independent and observed reflections	2008, 1018, 913	1991, 1140, 830	4985, 1955, 1165
Criterion for observed reflections	$I > 2\sigma(I)$	$I > 2\sigma(I)$	$I > 2\sigma(I)$

Table 1 (continued)

	β at 120 K	β at room temperature	β at 375 K
R_{int}	0.015	0.041	0.061
θ_{max} (°)	27.3	27.2	31.4
Range of h, k, l	$-4 \Rightarrow h \Rightarrow 2$ $-13 \Rightarrow k \Rightarrow 12$ $-14 \Rightarrow l \Rightarrow 17$	$-4 \Rightarrow h \Rightarrow 3$ $-13 \Rightarrow k \Rightarrow 7$ $-18 \Rightarrow l \Rightarrow 18$	$-2 \Rightarrow h \Rightarrow 5$ $-16 \Rightarrow k \Rightarrow 16$ $-21 \Rightarrow l \Rightarrow 21$
Refinement			
Refinement on	F^2	F^2	F^2
R $[F^2 > 2\sigma(F^2)]$, wR (F^2), S	0.038, 0.104, 1.05	0.073, 0.201, 1.19	0.078, 0.255, 1.16
No. of reflections	1018	1140	1955
No. of parameters	96	112	112
H-atom treatment	Mixture of independent and constrained refinement	Mixture of independent and constrained refinement	Mixture of independent and constrained refinement
Weighting scheme	$w = 1/[\sigma^2(F_o^2) + (0.0588P)^2 + 0.2706P]$, where $P = (F_o^2 + 2F_c^2)/3$	$w = 1/[\sigma^2(F_o^2) + (0.0639P)^2 + 0.63P]$, where $P = (F_o^2 + 2F_c^2)/3$	$w = 1/[\sigma^2(F_o^2) + (0.1467P)^2 + 0.0501P]$, where $P = (F_o^2 + 2F_c^2)/3$
$(\Delta/\sigma)_{max}$	0.004	0.005	0.022
$\Delta\rho_{max}$, $\Delta\rho_{min}$ (e Å^{-3})	0.199, −0.265	0.180, −0.178	0.26, −0.21
Extinction method	*SHELXL*97	*SHELXL*97	*SHELXL*97
Extinction coefficient	0.015 (6)	0.019 (9)	0.05 (3)

Computer programs used: *SHELXL*97 (Sheldrick, 1997), *KM4CCD* software (Kuma Diffraction, 1999), *SHELXS*97 (Sheldrick, 1990), *ORTEP*3 (Johnson *et al.*, 1997).

(Wójcik *et al.*, 2005). The comparison was aimed at providing some general conclusions concerning the interactions in nitrophenols. The crystal structures of *p*-nitrophenol and *m*-nitrophenol are deposited in the Cambridge Crystallographic Database under the NITPOL and MNPHOL refcodes.

The polymorphism of *p*-nitrophenol seems to be a thoroughly studied phenomenon. Since the papers of Coppens and Schmidt (Coppens & Schmidt, 1965*a*,*b*), the crystal structures of the polymorphs α and β have been known and the differences in their molecular packing known. Also, the possible mechanism of a topochemical photoreaction occurring in the light-unstable α polymorph, as a result of irradiation with visible light, has been discussed there. Recently, Kulkarni and co-workers (Kulkarni *et al.*, 1998; Kumaradhas *et al.*, 1999) performed the detailed X-ray diffraction investigation of charge-density distributions in polymorphs α and β and, additionally, in the irradiated α crystal. Their results indicate a relevant difference of the charge-density distribution and the molecular dipole moment between the polymorphs. The α polymorph after irradiation shows the charge-density distribution that is intermediate between those occurring in two polymorphs, and exhibits a distinctly smaller value of the molecular dipole moment than in the non-irradiated α and β crystals.

Both polymorphs crystallize in a centrosymmetric space group of the monoclinic crystallographic system. The molecules are linked by intermolecular hydrogen bonds between the hydroxyl and nitro group, forming infinite molecular chains. The polymorphs exhibit a different mutual orientation of the molecules in the chains. In the β crystal they are oriented co-linearly and the angle between molecular planes is $\sim 28°$. In the α crystal the molecules are oriented in a herringbone way and the angle between the benzene-ring plane of adjacent molecules in a chain is 74° (Coppens & Schmidt, 1965*a*,*b*). The hydrogen bonds are of comparable strength in both polymorphs because the O···O distance equals $\sim$ 2.821 Å in the α crystal and 2.828 Å in the β crystal at 120 K. The molecules are nearly planar – only the O atoms are very slightly displaced from the plane. Although the densities of the two crystals show very similar values, the density of the β polymorph is slightly larger, indicating that this is a stable form in the temperature range from liquid nitrogen up to ambient temperature. There is some ambiguity

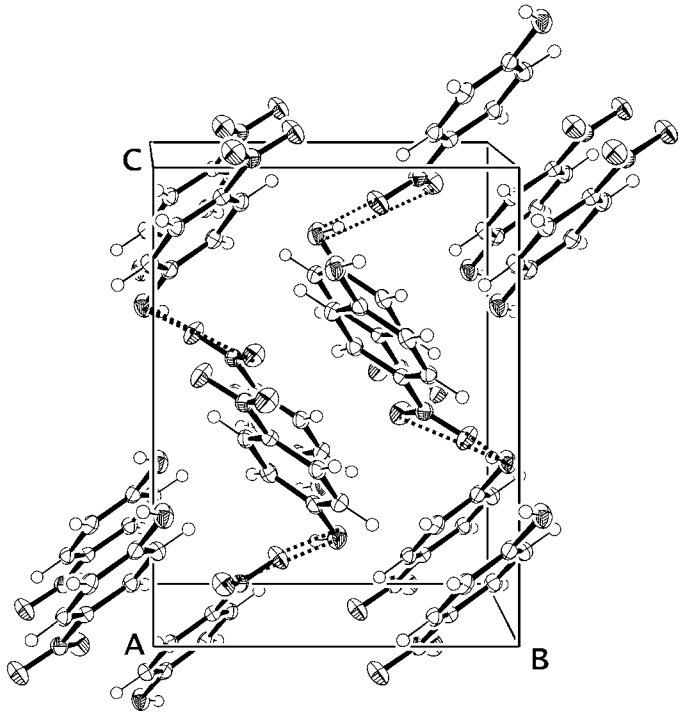

Figure 1
Molecular packing in the α polymorph of *p*-nitrophenol. The relevant short intermolecular distances are marked. The atomic displacement ellipsoids correspond to a 50% probability level.

Table 2
Thermal expansion coefficients (K^{-1}) in the α and β crystals calculated in the crystallographic axial system and in the thermal expansion principal axial system.

The ϕ angle is the angle between the α_1 and a^* axes in the counter-clockwise direction.

α			β		
$\alpha_{11} = 1.17 \times 10^{-5}$	0	$\alpha_{13} = 1.92 \times 10^{-5}$	$\alpha_{11} = 1.56 \times 10^{-4}$	0	$\alpha_{13} = -5.20 \times 10^{-6}$
0	$\alpha_{22} = 5.64 \times 10^{-5}$	0	0	$\alpha_{22} = 1.51 \times 10^{-5}$	0
$\alpha_{31} = 1.92 \times 10^{-5}$	0	$\alpha_{33} = 1.15 \times 10^{-4}$	$\alpha_{31} = -5.20 \times 10^{-6}$	0	$\alpha_{33} = 3.69 \times 10^{-5}$
$\alpha_1 = 8.20 \times 10^{-6}$	0	0	$\alpha_1 = 1.57 \times 10^{-4}$	0	0
0	$\alpha_2 = 5.64 \times 10^{-5}$	0	0	$\alpha_2 = 1.51 \times 10^{-5}$	0
0	0	$\alpha_3 = 1.19 \times 10^{-4}$	0	0	$\alpha_3 = 3.67 \times 10^{-5}$
$\phi = 10.15^\circ$			$\phi = 2.47^\circ$		

in the space-group choice for the two polymorphs. Coppens and Schmidt described the structures in the $P2_1/a$ (form β) and $P2_1/n$ (form α) space groups. Kulkarni *et al.* (1998) chose the $P2_1/n$ space group for the β polymorph and the $P2_1/c$ space group for the α crystal. This choice has an advantage as in both polymorphs the chains of hydrogen-bonded molecules are situated along the [101] direction. In this work we have adopted Kulkarni's space groups.

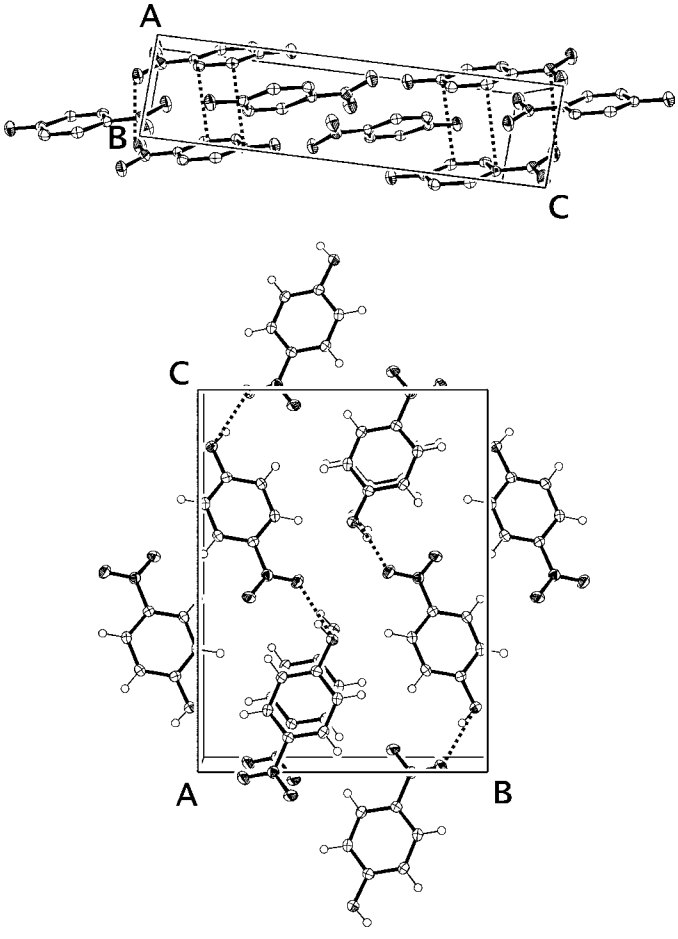

Figure 2
Molecular packing in the β polymorph of *p*-nitrophenol. The relevant short intermolecular distances are marked. The atomic displacement ellipsoids correspond to a 50% probability level.

As to the thermodynamic relationship between polymorphs, the authors cited determined that the β polymorph transforms into α on mild heating (Kulkarni *et al.*, 1998).

The α crystal's colour change from yellow to red after irradiation with visible light has been beyond the scope of this work. Nevertheless, we have been studying α crystals before and after irradiation and colour change. The differences of crystal structures and molecular dynamics between them are minor and border on the precision of the method. Hence, we decided to only present and analyse the results referring to non-irradiated crystals.

2. Experimental

Commercial *p*-nitrophenol was further purified by recrystallization and multiple zone melting. Single crystal specimens of the α and β forms were grown from dichlorobenzene and aqueous solutions, respectively. Their crystal habits were as described by Coppens & Schmidt (1965*a*,*b*): needles of the β form and thin, elongated plates of the α form.

X-ray diffraction measurements were performed on a KUMA Diffraction KM4CCD four-circle automatic diffract-

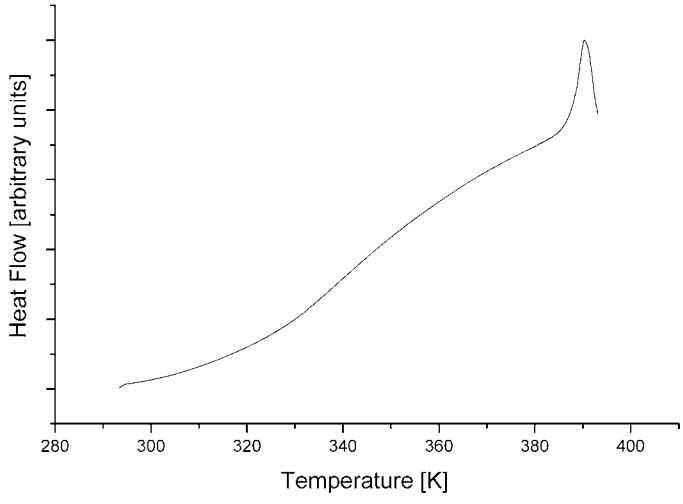

Figure 3
The DSC heating curve showing the endothermic effects of the $\beta \Rightarrow \alpha$ transformation and the melting. The heating rate was 10 K min^{-1}.

ometer equipped with an area detector and an Oxford Cryosystem cooling unit. Mo $K\alpha$ radiation (λ = 0.71073 Å) was used. The measurements were performed at several temperatures over the 120–375 K range for the β crystals and between 120 and 333 K for the α crystals. The precision of the temperature stability was 0.1 K. *Several single-crystal specimens were used in the experiments*. During the data collection ω scans were performed. No absorption corrections were used. Data reductions were carried out with KUMA *KM4CCD* software (Kuma Diffraction, 1999). The structures were solved by direct methods (Sheldrick, 1990) and refined by least-squares with the *SHELXL*97 package (Sheldrick, 1997). Atomic scattering factors were taken from the *International Tables for Crystallography* (1992, Vol. C, Tables 4.2.6.8 and 6.1.1.4). The H atoms were refined isotropically. Molecular graphics was carried out using *ORTEP*3 (Johnson *et al.*, 1997) and *MERCURY* (Bruno *et al.*, 2002). Other details of the data collection and the refinement for three temperatures from the range covered by the experiment are shown in Table 1.[1] Figs. 1 and 2 show the molecular packing in α and β crystals, respectively.

A rigid-body analysis (Cruickshank, 1956; Schomaker & Trueblood, 1968; Dunitz & White, 1973), including the correlation of the internal motion of the non-rigidly attached rigid group (Dunitz *et al.*, 1988; Schomaker & Trueblood, 1998), was carried out using *THMA*11 (Farrugia, 1999).

The differential scanning calorimetry (DSC) measurements were performed on a DSC7 Perkin-Elmer apparatus. The heating and cooling runs over a temperature range between 233 and 393 K were measured with different scanning rates. Several α and β samples weighed from 9 to 39 mg. Temperature was calibrated on the melting temperature of indium and cyclohexane. The energy effects were calibrated on the melting enthalpy of indium.

3. Results

3.1. Enantiotropic relationship between the α and β polymorphs

The X-ray diffraction experiment did not reveal any transformation of the β crystal's specimens up to 375 K, as may be seen in Table 1. However, an observation of α and β samples on the hot-stage microscope indicated that on heating the β crystals underwent an apparently first-order transformation coupled with the destruction of the crystals. This transformation could not be reversed on cooling. The crystals corresponded to the α form after transformation. The transformation occurred at a temperature between 331 and 366 K for different samples. Evidently, the occurrence of the transformation depended on the number of defects in a crystal. This rationalizes the absence of the $\beta \Rightarrow \alpha$ transformation during the high-temperature X-ray experiment due to the overheating of the β crystals. The DSC heating and cooling curves were irreproducible and depended on the samples. The transformation was manifested through a broad endothermic peak with the onset at a temperature from the range reported above. Sometimes no transformation was observed. An example of a DSC heating curve is shown in Fig. 3. Analysis of the numerous curves concluded that the β crystals melted at 384 ($\pm$1) K and α crystals melted at 381 ($\pm$1) K. The $\beta \Rightarrow \alpha$ transformation was very sluggish and thus difficult to analyse quantitatively. Nevertheless, a crude estimation indicated that the transition enthalpy was close to $\sim$5 kJ mol^{-1}. The enthalpy of melting amounted to $\sim$ 12 kJ mol^{-1}.

The phase situation in *p*-nitrophenol, depicted above, turns out to be quite similar as in *m*-nitrophenol. The orthorhombic polymorph of *m*-nitrophenol, stable at ambient temperature, and the metastable, monoclinic polymorph also stay in an enantiotropic relationship. The orthorhombic to monoclinic transformation occurs at 350 K and it is also irreversible on cooling. The enthalpy of the transition is minor (about 0.2 kJ mol^{-1}), reflecting the high level of isostructurality of the polymorphs. The melting of the high-temperature monoclinic polymorph occurs at 370 K with the enthalpy of melting amounting to $\sim$ 20 kJ mol^{-1} (Wójcik & Marqueton, 1989). This value may be compared with the sum of the enthalpies of the phase transition and melting found for *p*-nitrophenol. The lower value of the melting temperature of *m*-nitrophenol corresponds to slightly weaker intermolecular hydrogen bonds compared with *p*-nitrophenol.

3.2. Thermal expansion

The thermal expansion tensor depicts well the anisotropic interactions in a crystal. Figs. 4 and 5 show the relative increase of lattice parameters for polymorphs α and β, respectively. The thermal expansion curves corresponding to the two polymorphs are distinctly different, reflecting the different molecular interactions in the crystals. Thermal expansion coefficients are tensorial values (second-rank symmetric tensor) and their orientation in a crystal results from the crystal symmetry. In the case of monoclinic crystals

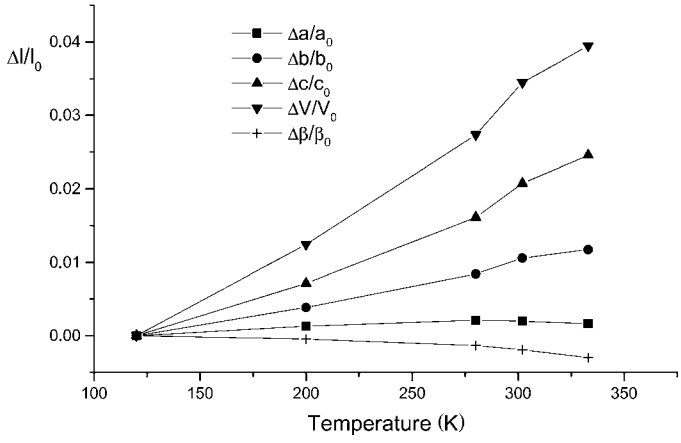

Figure 4
The relative increase of the α crystal parameters as a function of temperature.

[1] Supplementary data for this paper are available from the IUCr electronic archives (Reference: NS0011). Services for accessing these data are described at the back of the journal.

Table 3
The elements of **T** (translation), **L** (libration) and **S** (correlation between translations and librations) tensors in the inertial axes coordinate system for the α and β crystals (at chosen temperatures).

		α			β		
		120 K	Room temperature	333 K	120 K	Room temperature	375 K
T (Å^2)	T^{11}	0.02194	0.05473	0.06465	0.02089	0.04701	0.06028
	T^{12}	−0.00103	0.00131	−0.00097	0.00018	−0.00456	−0.00545
	T^{13}	0.00140	0.00461	0.00512	−0.00042	0.00134	−0.00124
	T^{22}	0.01803	0.04462	0.05271	0.01637	0.04012	0.05478
	T^{23}	0.00025	−0.00221	0.00225	−0.00090	−0.00110	−0.00120
	T^{33}	0.01195	0.03608	0.04224	0.01228	0.03584	0.04637
L (deg^2)	L^{11}	18.625	49.086	55.275	12.382	36.387	56.538
	L^{12}	1.310	−4.141	6.518	0.769	5.134	4.643
	L^{13}	0.264	−1.737	0.194	−0.132	1.420	3.346
	L^{22}	8.119	22.725	26.080	7.039	18.559	27.727
	L^{23}	−1.270	3.982	−4.756	−0.971	−2.891	4.137
	L^{33}	4.089	12.664	14.937	3.318	11.425	16.777
S (rad × Å)	S^{11}	0.00007	0.00062	0.00070	0.00029	0.00060	−0.00043
	S^{12}	0.00059	0.00214	−0.00156	0.00037	0.00097	0.00257
	S^{13}	−0.00066	0.00172	0.00098	0.00046	0.00203	−0.00171
	S^{21}	0.00050	0.00157	−0.00132	0.00030	0.00093	0.00160
	S^{22}	−0.00049	0.00101	0.00131	−0.00039	−0.00105	−0.00003
	S^{23}	0.00092	0.00254	−0.00273	0.00096	0.00286	−0.00453
	S^{31}	0.00013	0.00004	−0.00007	−0.00003	0.00032	−0.00014
	S^{32}	0.00040	0.00057	−0.00057	−0.00039	−0.00190	0.00395
	S^{33}	0.00042	−0.00163	−0.00201	0.00010	0.00046	0.00046
wR†		0.085	0.039	0.026	0.074	0.053	0.040

† $wR = [\Sigma w(U_o^{ij} - U_c^{ij})^2 / \Sigma w(U_o^{ij})^2]^2$; $w = \sigma[\langle U_o^{ij} \rangle]^{-2}$.

the relative increase of the b parameter corresponds to the principal α_2 coefficient. The α_1 and α_3 principal coefficients correspond to the thermal expansion along directions which are mutually perpendicular and lying in the plane that is orthogonal to the b axis. The α_1 and α_3 values may be calculated through diagonalization of the matrix, whose elements correspond to the thermal expansion coefficients calculated in the crystallographic axial system. The coefficients are calculated using mathematical algorithms given, for example, by Cole (Cole *et al.*, 2000). In this work a linear dependence of the increase in the relative parameters on temperature was assumed for the α crystals in the whole temperature range covered by the experiment, and from 120 to 311 K for the β crystals. The coefficients were calculated as derivatives $(\partial l/l_o \partial T)$. Table 2 reports the elements of the thermal expansion tensor calculated in the crystallographic axial system and in the thermal expansion principal axial system. The curves shown in Figs. 4 and 5, as well as the values from Table 2, indicate that intermolecular interactions are essentially different in polymorphs α and β. In the α crystals the smallest thermal expansion occurs along the direction closest to the direction of the intermolecular hydrogen bonds. The largest thermal expansion coefficient, α_3, corresponds to a direction perpendicular to the α_1 axis. In the β crystals the largest thermal expansion occurs along the direction of the stacks of overlapping molecules, *i.e.* along the a^* axis, while the thermal expansion in the plane perpendiclar to the a^* axis is minor.

These results are in line with the structures of the studied crystals. The two polymorphs realise two main types of molecular packing in organic crystals: stacking and herringbone arrangements. Molecules in the β crystal are arranged in stacks along the a axis with the distance between molecular planes equal to 3.36 Å (at 120 K). The arrangement is similar to that in *m*-dinitrobenzene. The crystals of *m*-dinitrobenzene and β *p*-nitrophenol show two-dimensional isostructurality and the elements of their thermal expansion tensors have similar values. The principal thermal expansion coefficients calculated for *m*-dinitrobenzene are 4.14, 5.45 and 13.8 10^{-5} K^{-1} (Wójcik *et al.*, 2002). Such a stacking arrangement is characteristic for highly polarizable planar molecules (Desiraju, 1989), *e.g.* hexachlorobenzene (Brown & Strydom, 1974).

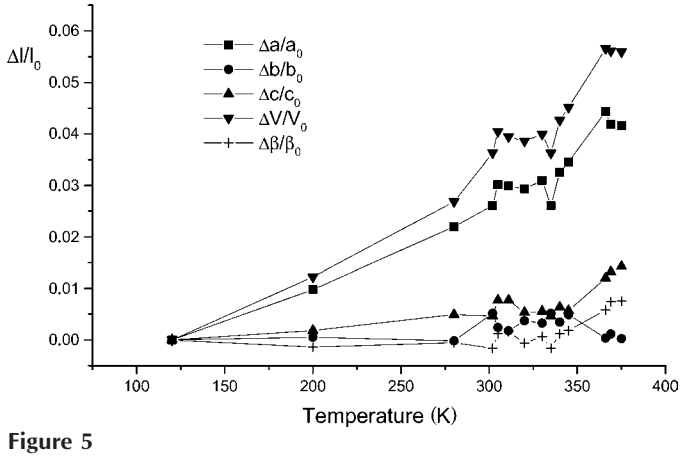

Figure 5
The relative increase of the β crystal parameters as a function of temperature.

Molecules in the α crystals are arranged in a herringbone pattern, which is characteristic for hydrogen-bonded molecules forming molecular chains (Desiraju, 1989). The molecular arrangement resembles (to some extent) the monoclinic polymorph of *m*-nitrophenol with the overlapping of centrosymmetrically related molecules from adjacent molecular chains. The distance between the molecular planes in such a dimer amounts to 3.373 Å (at 120 K). The thermal expansion tensors of the two crystals also exhibit similar features. The principal thermal expansion coefficients calculated for monoclinic *m*-nitrophenol at 150 K are: −0.18, 7.88 and 7.20 10^{-5} K^{-1} (Wójcik *et al.*, 2005).

3.3. Rigid-body analysis of the anisotropic displacement parameters with a correlation of the internal torsion of the nitro group

Atomic anisotropic displacement parameters may be analysed in terms of the TLS formalism under the condition that the amplitudes of the internal (atomic) vibrations are negligible compared with the amplitudes of the whole-molecule motions. This method, also called a rigid-body approximation, uses the atomic displacement parameters to calculate the elements of the molecular libration (**L**), translation (**T**) and screw (**S**) tensors (Cruickshank, 1956; Schomaker & Trueblood, 1968; Dunitz & White, 1973). The internal vibrations of large amplitude (for nitrophenol this is the torsional vibration of the nitro group) may be correlated with the molecular librations and translations (Dunitz *et al.*, 1988; Schomaker & Trueblood, 1998). The results of the rigid-body analysis provide the values of the mean-square amplitudes of molecular libration and translation (six values of the second-rank tensors) and nine values of the **S** tensor representing the correlation between librations and translations in non-centrosymmetric molecules. Additionally, the $(\varphi^2 + 2\lambda^{\parallel}\varphi)$ value may be calculated, where φ denotes the amplitude of the torsional vibration of the non-rigidly attached rigid group (the nitro group in the case of nitrophenol) and $\lambda^{\parallel}$ is the amplitude of the librational vibration of this group about the same axis. The calculated $(\varphi^2 + 2\lambda^{\parallel}\varphi)$ value may be treated as the amplitude of the overall motion of the nitro group about the C—N bond direction and may be compared with $\lambda^{\parallel}$, *i.e.* the contribution to the motion from molecular libration.

The results of the rigid-body analysis performed for the α and β crystals as a function of temperature are shown in Fig. 6. Fig. 7 shows a *p*-nitrophenol molecule with inertial axes I_1, I_2 and I_3 corresponding to the librations L_1, L_2 and L_3, respectively. The thermal dependence of the amplitudes of the nitro-group vibration (overall and the librational contribution) in the α and β crystals is shown in Fig. 8. Table 3 reports the elements of the **T**, **L** and **S** tensors calculated for the two polymorphs in the inertial axes coordinate system. The values of the *R* factor calculated for three chosen temperatures indicate that the rigid-body approximation is valid for the α and β crystals in this temperature range.

Analysis of the results from Fig. 6–8 and Table 3 reveals the difference in molecular interactions between the polymorphs. The α polymorph, metastable up to $\sim$331 K, exhibits distinctly larger amplitudes of molecular motions. Especially

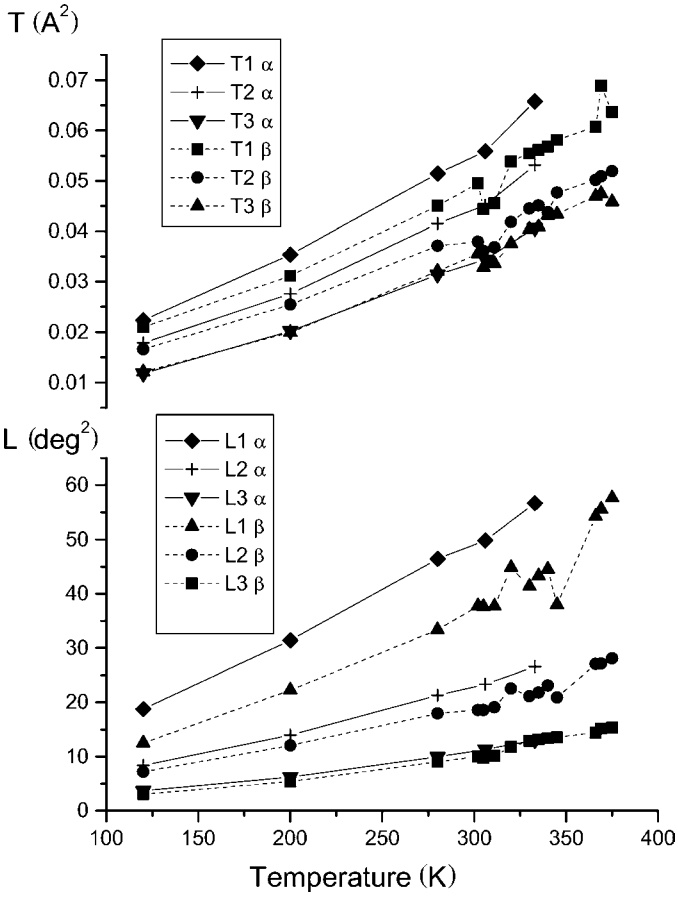

Figure 6
The **T** and **L** eigenvalues and their thermal evolution in the α and β crystals. The lines serve as guides to the eye.

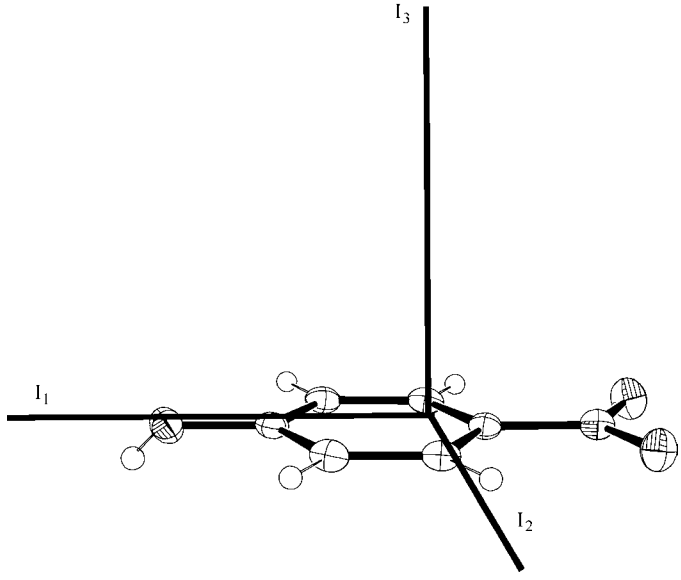

Figure 7
The *p*-nitrophenol molecule with the inertial axes.

the libration L_1 about the axis of the smallest inertial moment (I_1), being the largest in both crystals, is far more pronounced in the α polymorph. On the other hand, the nitro group torsional vibrations are more pronounced in the β crystal, as seen in Fig. 8. Such a distribution of vibrational energy between internal and lattice modes as in the α and β polymorphs had also been observed in the case of two polymorphs (metastable monoclinic and stable orthorhombic) of *m*-nitrophenol (Wójcik *et al.*, 2005).

4. Molecular packing in the α and β polymorphs and its influence on photo- and thermo-stability

Molecular packing in the α and β polymorphs, although discussed in detail in the papers of Coppens (Coppens & Schmidt, 1965*a*,*b*) and Kulkarni (Kulkarni *et al.*, 1998), is worth some additional remarks. The arrangements of the molecules, apparently different in the polymorphs, result from competition between interactions within molecular chains and stacks. The attractive interactions between hydroxyl and nitro groups, as hydrogen-bond donors and acceptors, lead to molecular chains in both polymorphs. This is a typical molecular arrangement in nitrophenols and nitroanilines (Panunto *et al.*, 1987) and also occurs in both polymorphs of *m*-nitrophenol. On the other hand, the interactions between molecular dipoles result in centrosymmetric molecular dimers of overlapped molecules. They also occur in the α polymorph of *p*-nitrophenol, as in the monoclinic form of *m*-nitrophenol (Wójcik *et al.*, 2005). The β polymorph, although centrosymmmetric, reveals another arrangement of molecular chains. Namely, the stacks of translationally equivalent molecules along the *a* crystallographic axis occur in the crystal and they are similar to the stacks along the *c* axis in the isostructural crystal of *m*-dinitrobenzene. In *m*-dinitrobenzene the stacks of translationally equivalent molecules seem to be stabilized by interactions between highly polar nitro groups exhibiting large amplitude, out-of-plane torsional vibrations. (Wójcik *et al.*, 2002).

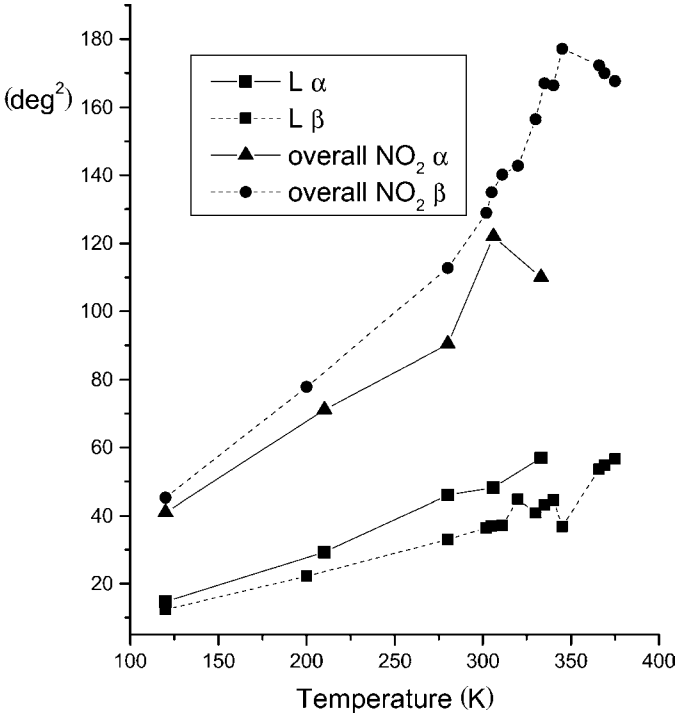

Figure 8
The mean-square overall motion amplitudes and the mean-square libration amplitudes (denoted as **L**) of the nitro group about the C—N bond in the α and β crystals. The lines serve as guides to the eye.

The α polymorph may be compared with the high-temperature monoclinic form of *m*-nitrophenol. In both crystals the ribbons of hydrogen-bonded molecules are arranged in a head-to-tail fashion and every two molecules from adjacent ribbons overlap, forming a centrosymmetric dimer. The average distance between the overlapping molecules is ~ 3.4 Å in both crystals. The photosensitivity of the α polymorph in contrast to the monoclinic *m*-nitrophenol may result from different electron conjugation along the hydrogen-bonded molecules. In *m*-nitrophenol the molecular ribbons are formed by coplanar molecules. Thus, the through-conjugation should be pronounced. In *p*-nitrophenol the hydrogen-bonded molecules are not coplanar. In the α polymorph the through-conjugation along the molecular chains seems to be reduced, because the adjacent molecules form an angle of $\sim 74^\circ$. Thus, the α polymorph may be treated as built of charge-transfer complexes of overlapped molecules exhibiting a charge-transfer absorption band in the visible range of electromagnetic radiation (Rohleder, 1964). The pronounced decrease of the molecular dipole moment (from 18 to 9.9 D) in the α crystal after irradiation, and colour change (Kumaradhas *et al.*, 1999) corroborate the above statement. On the other hand, the extremely high values of the molecular dipole moments in the α and β crystals (about 20 D) compared with the corresponding value calculated for a free molecule (~ 5.5 D; Kulkarni *et al.*, 1999) seem to also originate from a lack of through-conjugation along the molecular chains. In orthorhombic *m*-nitrophenol the molecular dipole moment has a value of ~ 7.8 D, which is only slightly larger than that calculated for a free molecule (Hamzaoui *et al.*, 1996; Wójcik *et al.*, 1996). The electron through-conjugation along the hydrogen-bonded coplanar molecules seems to account for the effect in *m*-nitrophenol.

The enantiotropic relationship between the α and β polymorphs is not very different from the enantiotropy of the *m*-nitrophenol polymorphs. The orthorhombic to monoclinic transformation in *m*-nitrophenol also occurs at a temperature above ambient. The high-temperature monoclinic form also stays outside the range of its thermodynamic stability as a metastable phase. It may be obtained from solution, together with the other polymorph as a concomitant polymorph (Bernstein *et al.*, 1999). The α and β polymorphs may also be obtained from the same solution, so they may also be called concomitant polymorphs. The persistent metastability of the α crystals corresponds to the similar thermodynamic situation of the high-temperature form of *m*-nitrophenol. The lasting metastability of the α form of *p*-nitrophenol and of the monoclinic form of *m*-nitrophenol originates probably from interactions within the centrosymmetric dimers of overlapping

molecules. In monoclinic *m*-nitrophenol the interactions are as strong as interactions between the hydrogen-bonded molecules, as was recently calculated using the quantum-chemical method. The interactions between the overlapped molecules account for damping the out-of-plane torsional vibrations of the nitro group which trigger the phase transition in *m*-nitrophenol (Wójcik *et al.*, 2005).

5. Conclusions

The phase transition in *p*-nitrophenol is driven by thermal librations, coupled with strongly increasing torsional vibrations of the nitro groups, about the axes of the molecular chains. The reverse transition does not occur due to the dampened torsional vibrations of the nitro groups in the high-temperature form. The mechanism of the β to α phase transition seems to be similar to that in *m*-nitrophenol (Wójcik *et al.*, 2005).

The question arises as to why two polymorphs of *p*-nitrophenol exhibit relatively different molecular arrangements, whereas two polymorphs of *m*-nitrophenol are isostructural in three dimensions. The other question, that results from the previous one, is: to what extent are the structures of the stable forms of *p*-nitrophenol and *m*-nitrophenol and their metastable forms, respectively, similar?

Fig. 9 shows the two nearest neighbours in the four crystals under consideration. In the stable forms of *p*- and *m*-nitrophenols these are two molecules joined by the hydrogen bond and two molecules overlapped in a parallel fashion. In the metastable forms the hydrogen-bonded molecules also occur but two molecules are overlapped in an antiparallel fashion.

The crystallization of a polymorph occurs during a nucleation process. A nucleus may not correspond to the most stable form for the thermodynamic conditions given. Then, it may, or not, transform to a more stable form (Bernstein, 2002). The transformation is kinetically controlled and its rate depends on the activation energy. Evidently, the activation barrier is also high between the *p*-nitrophenol and *m*-nitrophenol polymorphs. Analysing the crystal structures and interactions in the *m*-nitrophenol polymorphs with quantum-chemical methods we found that the strongest attractive interactions in the low-temperature orthorhombic form occur between hydrogen-bonded molecules in a chain (Wójcik *et al.*, 2005). It is quite probable that this is true for the β polymorph of *p*-nitrophenol. Thus, an initial nucleation of the stable polymorphs of both compounds refers to the molecules linked by intermolecular OH···ON hydrogen bonds. Then such linear aggregates arrange and grow, forming crystals of the β *p*-nitrophenol or the orthorhombic *m*-nitrophenol. In the metastable form of *m*-nitrophenol the attractive interactions within centrosymmetric dimers of overlapping molecules are as strong as interactions between hydrogen-bonded molecules (Wójcik *et al.*, 2005). Assuming that this is also true for the α polymorph of *p*-nitrophenol we may presume that the nucleation of the metastable forms of both compounds is initiated through an overlapping of two molecular dipoles in a head-to-tail manner. Then, such a centrosymmetric dimer is involved in OH···ON hydrogen bonds leading to molecular chains. Thus, the crystallization of the concomitant polymorphs of both nitrophenol isomers is realised on a molecular level. The persistent metastability of the high-temperature polymorphs seems to result from relatively strong interactions between overlapped molecules, forming centrosymmetric dimers.

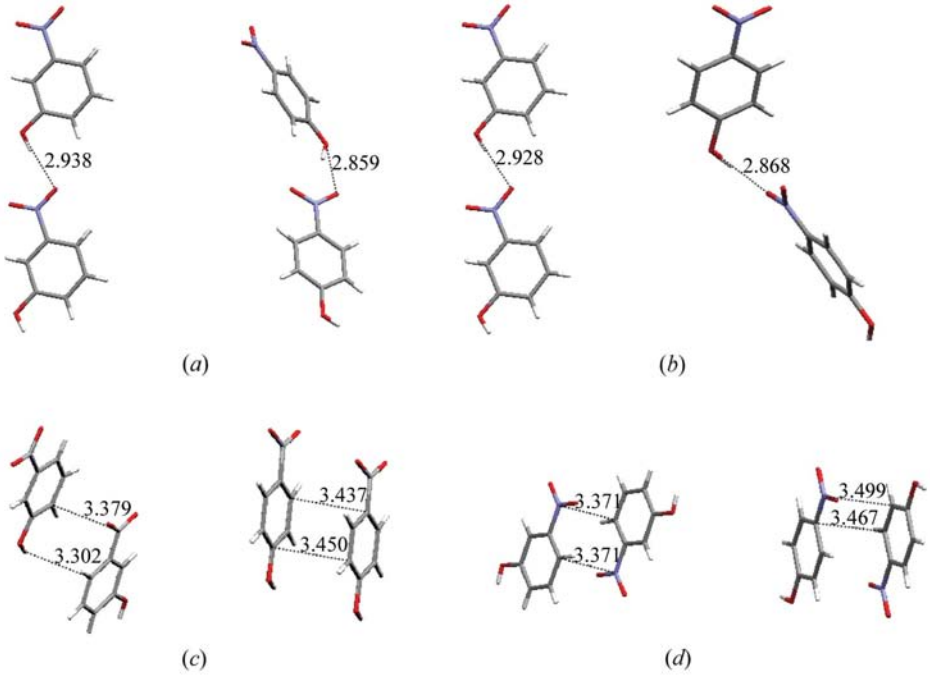

Figure 9
The molecular dimers corresponding to the strongest intermolecular interactions in the polymorphs of *p*- and *m*-nitrophenol. (*a*) Two hydrogen-bonded molecules in the stable polymorphs of *m*-nitrophenol (orthorhombic form) and *p*-nitrophenol (β form); (*b*) two hydrogen-bonded molecules in the metastable polymorphs of *m*-nitrophenol (monoclinic form) and *p*-nitrophenol (α form); (*c*) two overlapped molecules in the stable polymorphs of *m*-nitrophenol (orthorhombic form) and *p*-nitrophenol (β form); (*d*) two overlapped molecules in the metastable polymorphs of *m*-nitrophenol (monoclinic form) and *p*-nitrophenol (α form).

References

Bernstein, J. (2002). *Polymorphism in Molecular Crystals*. Oxford: Clarendon Press.
Bernstein, J., Davey, R. J. & Henck, J.-O. (1999).

Angew. Chem. Int. Ed. **38**, 3440–3461.
Brown, G. M. & Strydom, O. A. W. (1974). *Acta Cryst.* B**30**, 801–804.
Bruno, I. J., Cole, J. C., Edgington, P. R., Kessler, M. K., Macrae, C. F., McCabe, P., Pearson, J. & Taylor, R. (2002). *Acta Cryst.* B**58**, 389–397.
Cole, J. M., Wilson, C. C., Howard, J. A. & Cruickshank, F. R. (2000). *Acta Cryst.* B**56**, 1085–1093.
Coppens, P. & Schmidt, G. M. J. (1965*a*). *Acta Cryst.* **18**, 62–67.
Coppens, P. & Schmidt, G. M. J. (1965*b*). *Acta Cryst.* **18**, 654–663.
Cruickshank, D. W. J. (1956). *Acta Cryst.* **9**, 754–756.
Desiraju, G. R. (1989). *Crystal Engineering, The Design of Organic Solids.* Amsterdam: Elsevier Science Ltd.
Dunitz, J. D., Maverick, E. F. & Trueblood, K. N. (1988). *Angew. Chem. Int. Ed. Engl.* **27**, 880–895.
Dunitz, J. D. & White, D. N. J. (1973). *Acta Cryst.* A**29**, 93–94.
Fábián, L. & Kalman, A. (2004). *Acta Cryst.* B**60**, 547–558.
Farrugia, L. (1999). *J. Appl. Cryst.* **32**, 837–838.
Hamzaoui, F., Baert, F. & Wójcik, G. (1996). *Acta Cryst.* B**52**, 159–164.
Johnson, C. K., Burnett, M. N. & Farrugia, L. J. (1997). *ORTEP*3. Windows Version. University of Glasgow, Scotland.
Kulkarni, G. U., Kumaradhas, P. & Rao, C. N. R. (1998). *Chem. Mater.* **10**, 3498–3505.
Kumaradhas, P., Srinivasa Gopalan, R. & Kulkarni, G. U. (1999). *Proc. Indian Acad. Sci. (Chem. Sci.)* **4**, 569–570.
Kuma Diffraction (1999). *Kuma KM4CCD Software*, Version 1.61. Kuma Diffraction, Wrocław, Poland.
Panunto, T., Urbańczyk-Lipkowska, Z., Johnson, R. & Etter, M. C. (1987). *J. Am. Chem. Soc.* **109**, 7786–7797.
Rohleder, J. (1964). Habilitation Thesis, Politechnika Wrocławska, Wrocław, Poland.
Schomaker, V. & Trueblood, K. N. (1968). *Acta Cryst.* B**24**, 63–76.
Schomaker, V. & Trueblood, K. N. (1998). *Acta Cryst.* B**54**, 507–514.
Sheldrick, G. M. (1990). *Acta Cryst.* A**46**, 467–473.
Sheldrick, G. M. (1997). *SHELXL*97. University of Göttingen, Germany.
Wójcik, G., Lipiński, J., Szostak, M. M. & Komorowska, M. (1996). *Adv. Mater. Opt. Electron.* **6**, 307–311.
Wójcik, G., Holband, J., Szymczak, J. J., Roszak, S. & Leszczynski, J. (2005). *Cryst. Growth Des.* In the press.
Wójcik, G. & Marqueton, Y. (1989). *Mol. Cryst. Liq. Cryst.* **168**, 247–254.
Wójcik, G., Mossakowska, I., Holband, J. & Bartkowiak, W. (2002). *Acta Cryst.* B**58**, 998–1004.